Designing Superoxide-Responsive Near-Infrared Afterglow Materials for Enhanced Arthritis Imaging

Shuai Huang [a], Shuaige Bai [a], Meihui Liu [a], Xueyan Huang [a,b], Jing Hou [a,c], Ting Luo [a], Yiyang Zhou [a], Shuang Huang [a], Wenbin Zeng *[a]

[a]. Xiangya School of Pharmaceutical Sciences, Central South University, Changsha 410013, China.

[b]. Department of Chemistry, Rice University, Houston 77005, USA.

[c]. Hunan Cancer Hospital & the Affiliated Cancer Hospital of Xiangya School of Medicine, Central South University, Changsha 410078, China.

General Information and Methods

Materials. The co-polymer DSPE-PEG2000 (1,2-distearoyl-sn-glycero-3-phosphoethanolamine-N- [methoxy (polyethylene glycol)-2000]) was purchased from J&K chemical Ltd. The chemicals and reagents for the synthesis including 3-Hydroxybenzaldehyde, tetrabutyl ammonium bromide (TBAB), trimethyl orthoformate, imidazole, TBDMSCl, trimethyl phosphite, lithium diisopropylammonium (LDA), adamantanone, tetrabutylammonium fluoride, polyformaldehyde, magnesium chloride, cyanomethyl triphenylphosphonium were purchased from J&K chemical Ltd., Tetrahydrofuran (THF) was distilled from sodium benzophenone ketyl under dry nitrogen immediately prior to use.

Characterization. NMR spectra were recorded using a Bruker AVANCE III 500 MHz spectrometer. High-resolution mass spectra (HRMS) of the compounds were recorded on a Varian 7.0 T FTMS. UV-vis absorption spectra were obtained on a Shimadzu Model UV-1700 spectrometer. Photoluminescence (PL) spectra were measured on a Perkin-Elmer LS-55 spectrofluorometer. The afterglow emission spectra of NPs were measured on 2 a spectrofluorometer (Edinburgh Instrument-FS5) without excitation. The average hydrodynamic diameter and size distribution of the samples were studied by dynamic light scattering (DLS) employing a 90 Plus analyzer (Brookhaven Instruments Co., USA) at a fixed angle of 90°. Transmission electron microscopy (TEM; JEM-2010F, JEOL, Japan) was employed to study the morphology of the NPs.

For both in vitro and in vivo, the afterglow imaging was conducted using an Xenogen IVIS Lumina II system in a bioluminescent mode without excitation, and NIR fluorescence imaging was conducted with the same IVIS instrument in a fluorescent mode with excitation at 500 nm. The immunofluorescent staining analysis was detected using a confocal laser scanning microscopy (Zeiss LSM 710)

Cell culture and cytotoxicity assay

4T1 mouse breast cancer cells were cultured in Roswell Park Memorial Institute (RPIM) 1640 medium supplemented with 10% fetal bovine serum (FBS), 100 μg/mL penicillin, and 100 μg/mL streptomycin in a humidified incubator containing 5% CO_2 at 37 °C.

Cell imaging in 4T1 cell lines

The cells were seeded into 6-well plates which have 5×10^5 cells per well and incubated for 24 h. Before imaging, the live cells were incubated with **APT/TTQ NPs** (25 μg/mL based on APT) for different periods and then washed with phosphate-buffered saline (PBS) three times. Subsequently, the cells were washed thoroughly and cell nuclei were stained with Hoechst 33342 (0.5 μg mL^{-1}). Fluorescence images were taken by NIKON ECLIPSE Ts2R inverted fluorescence microscope. Excited and detection was performed in a sequential mode under the following conditions: **APT/TTQ NPs** were excited at 560 nm, detected in the range from 550 to 660 nm; The cell nucleus stained with Hoechst 33342 were excited at 380 nm, detected at 420 nm.

Chemiluminescence and fluorescence imaging of LPS-induced inflammation mice model

All female BALB/c mice (8 weeks old) were purchased from Animal Center of Xiangya Medical School, Central South University. All animal experiments were performed according to the relevant ethical regulations of Central South University, and this study received approval from Xiangya School of Pharmaceutical Science, Central South University (2021-S027). To establish a lipopolysaccharide (LPS) induced inflammation

model, mice were injected subcutaneously with LPS (2 mg/mL) into the tibiotarsal joints of the mice. The mice were divided into two groups (n = 3), including (1) Subcutaneously injected with saline (50 μL) into the left tibiotarsal joints of the mice and then subcutaneously injected with LPS (2 mg/mL, 50 μL) into the right tibiotarsal joints of the mice. Five hours later, both the right and the left tibiotarsal joints of the mice were injected with NPs (100 μg/mL based on APT, 50 μL) and imaged by IVIS system. (2) Subcutaneously injected with saline (50 μL) into the left tibiotarsal joints of the mice and then subcutaneously injected with LPS (2 mg/mL, 50 μL) into the right tibiotarsal joints of the mice. Four and a half hours later, both the right and the left tibiotarsal joints of the mice were injected with Tiron (10 mmol/L, 50 μL). Half hours later, the same regions were injected with NPs (100 μg/mL based on APT, 50 μL) and imaged by IVIS system. Chemiluminescence intensity was recorded by IVIS bioluminescence with 60s of acquisition time under the open filter. For fluorescence imaging, the excitation wavelength was 500 nm, and the collected emission wavelength was 600-650 nm.

TTQ: Compound **19** (100 mg, 0.22 mM) was taken and dissolved in acetonitrile, iodomethane (70 mg, 0.5 mM) was added and refluxed for 12 hours. After that, the mixture was evaporated under vacuum and purified on a silica-gel column using MeOH/DCM (v/v 50:1 to 10:1) as eluent. Then a red solid was obtained in 40% yield. Compound **20** was then dissolved in methanol, saturated aqueous KPF6 solution was added and stirred at room temperature for 12 h and further purified by HPLC.

^{1}H NMR (500 MHz, DMSO-d6) δ = 9.40 (d, *J* = 6.5, 1H), 8.85 (d, *J* = 8.5, 1H), 8.53 (d, *J* = 8.8, 1H), 8.37 - 8.28 (m, 1H), 8.23 (d, *J* = 6.3, 1H), 8.15 - 8.07 (m, 1H), 8.02 (d, *J* = 4.0, 1H), 7.81 - 7.71 (m, 3H), 7.38 (t, *J* = 7.9, 4H), 7.20 - 7.08 (m, 6H), 7.02 (d, *J* = 8.7, 2H), 4.59 (s, 3H).^{13}C NMR (126 MHz, DMSO-d6) δ = 151.4, 149.5, 148.9, 148.8, 146.9, 139.6, 135.9, 135.5, 133.7, 130.7, 130.2, 128.3, 127.6, 126.1, 126.0, 125.4, 125.4, 124.5, 122.4, 121.0, 120.2, 45.3. HR-MS: Chemical Formula: $C_{32}H_{25}N_2S^+$, Exact Mass: 469.1733, found: 469.1690.

APT: 100 mg of compound **7**[1] was dissolved in THF and anhydrous pyridine (80 mg,

1 mM) was added slowly dropwise at -78°C. After stirring for 30 minutes, trifluorosulfonic anhydride (140 mg, 0.5 mM) was added slowly and stirring was continued for 30 minutes before transferring to room temperature and stirring was continued for 2 hours. After the reaction was complete, the reaction system was extracted with ethyl acetate, the organic phases were combined and the organic phase was dried with anhydrous magnesium sulfate. The product was then purified by silica gel column. 85 mg of **APT** was obtained

^{1}H NMR (600 MHz, $CDCl_3$) δ = 7.62 (d, *J*=8.2, 1H), 7.58 (d, *J*=16.6, 1H), 7.42 (d, *J*=8.2, 1H), 7.34 (d, *J*=1.2, 1H), 6.02 (d, *J*=16.6, 1H), 3.33 (s, 3H), 3.27 (s, 1H), 2.69 (s, 1H), 2.04 – 1.95 (m, 4H), 1.91 – 1.77 (m, 8H). ^{13}C NMR (151 MHz, $CDCl_3$) δ = 146.86, 141.90, 141.22, 141.01, 136.83, 129.28, 127.10, 125.53, 123.98, 123.45, 122.73, 119.60, 117.48, 117.31, 100.29, 58.38, 39.09, 39.01, 36.89, 32.40, 31.60, 30.65, 29.69, 29.59, 28.05.

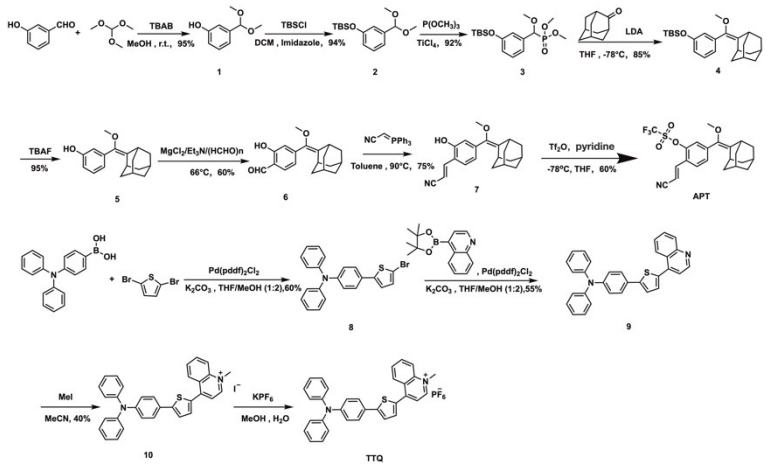

Scheme 1. Synthetic routes to the compounds **APT** and **TTQ**.

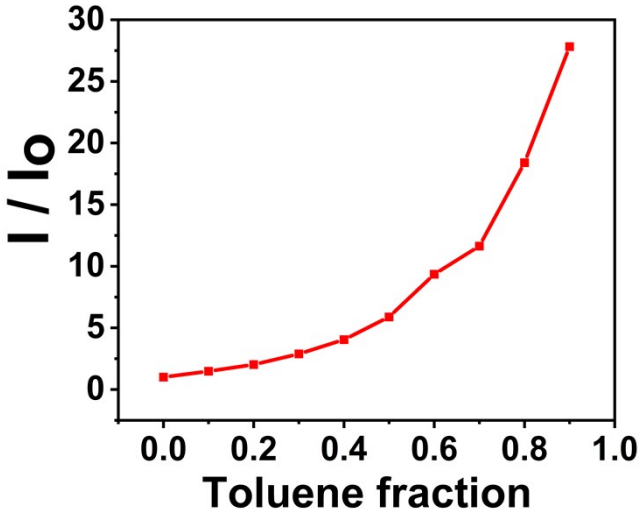

Fig S1. Trends in the AIE phenomenon of **TTQ**.

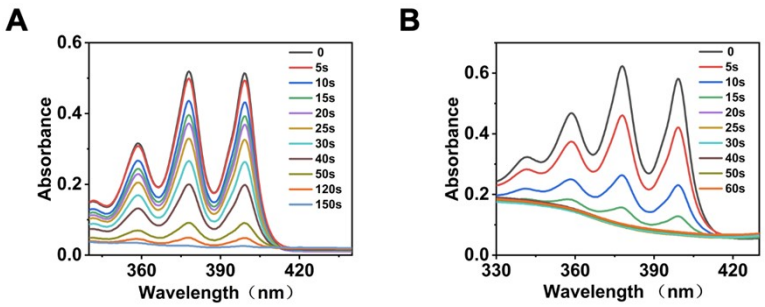

Fig S2. Absorption spectrum of ABDA (50 μM) in the presence of (A) RB (10 μM) (B) **TTQ** (10 μM) under different light time.

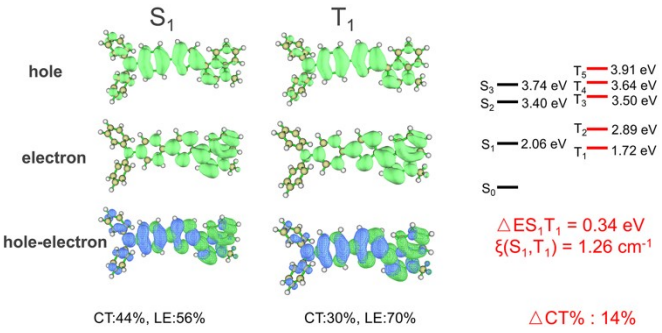

Fig. S3 Hole-Electron analyses of TTQ in the S1 and T1 states and the corresponding CT/LE ratios. Energy levels of TTQ in the S and T states as well as the energy level difference between S1 and T1 and the SOC values.

Table S1. Absorption values at different calculation levels and experimental absorption

values

Compound	B3LYP/def2-TZVP	PBE0/def2-TZVP	CAM-B3LYP/def2-TZVP	M062-X/def2-TZVP	EXP
TTQ	1.7958 eV, 690.42 nm	1.9292 eV, 642.66 nm	2.5779 eV, 480.95 nm	2.4960 eV, 496.73 nm	2.43 eV, 510 nm

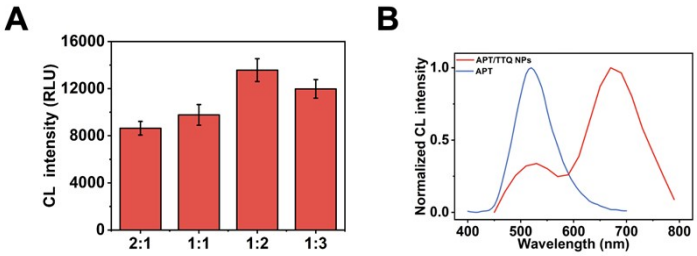

Fig. S4 (A) Chemiluminescence intensity of nanoparticles prepared at different **TTQ** to **APT** ratios triggered by KO_2 after light exposure. (B) Chemiluminescence spectra of **APT** and **APT/TTQ NPs** (2:1).

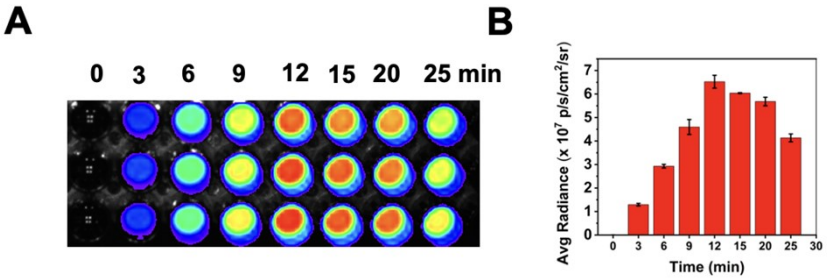

Fig. S5 Intensity of chemiluminescence activated by KO_2 in **APT/TTQ** NPs at different light times.

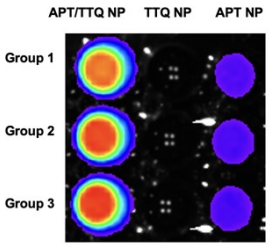

Fig. S6 Afterglow images showing the maximal afterglow intensities of various NPs in with KO_2 at 37 °C post white light pre-irradiation.

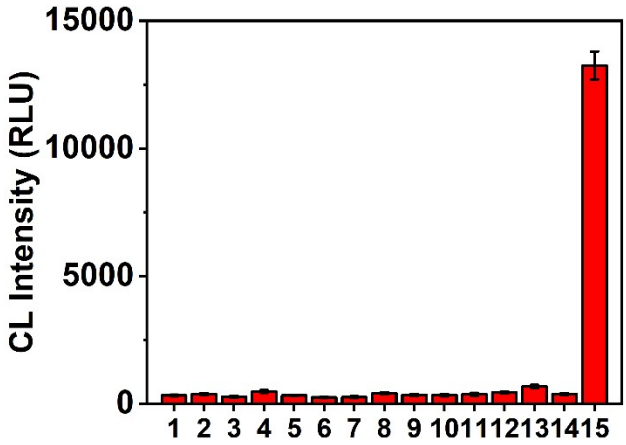

Fig. S7 Chemiluminescence selectivity study of **APT/TTQ NPs** for different substances. (1) Blank, (2) $FeCl_3$, (3) $ZnCl_2$, (4) $FeCl_2$, (5) AgCl, (6) Na_2CO_3, (7) $NaHCO_3$, (8) KCl, (9) NaCl, (10) $AlCl_3$, (11) $CaCl_2$, (12) $MgCl_2$, (13) Na_2SO_4, (14) GSH, (15) KO_2.

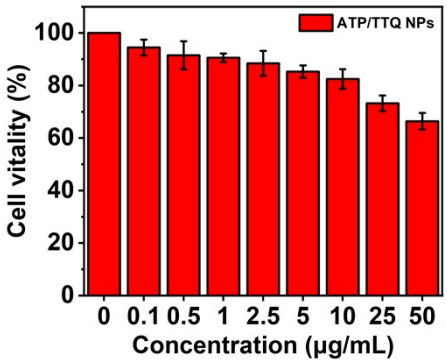

Fig. S8 Toxicity studies of **APT/TTQ** NPs on 4T1 cells.

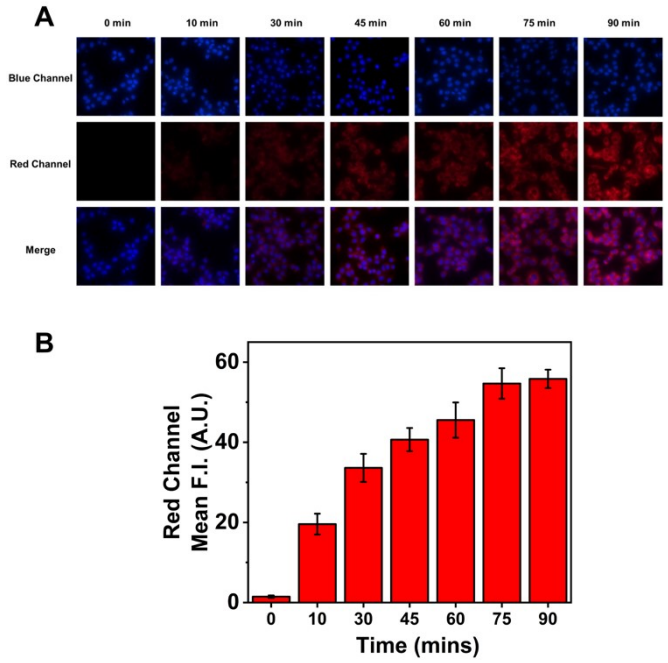

Fig. S9 Inverted fluorescence images and (B) MFI of 4T1 cells treated with APT/TTQ NPs (10 μg / mL) for 90 min. Red fluorescence indicates APT/TTQ NPs, and blue fluorescence indicates Hoechst 33342 that was used to stain the nucleus

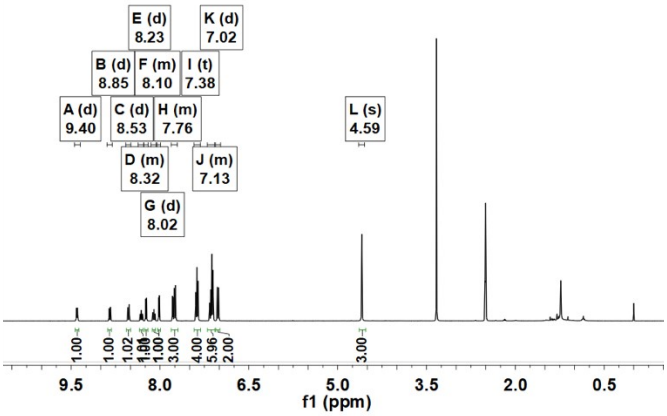

Fig. S9. ^{1}H NMR spectrum of **TTQ** in DMSO-d_6.

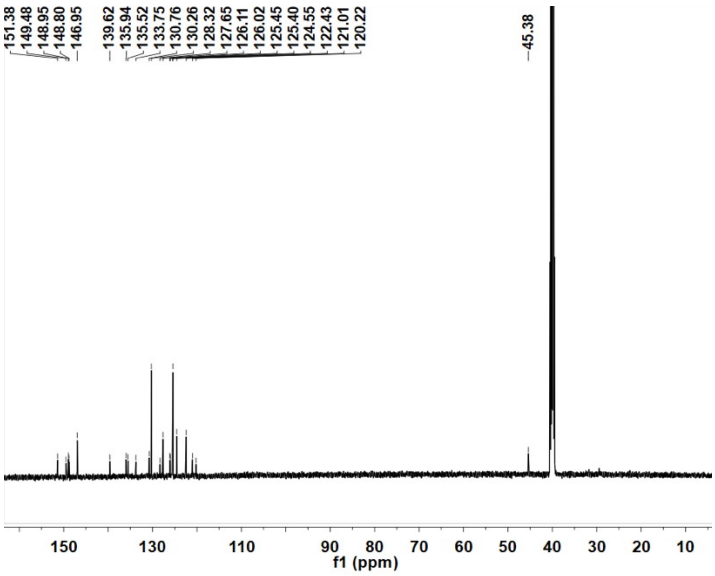

Fig. S10. ^{13}C NMR spectrum of **TTQ** in DMSO-d_6.

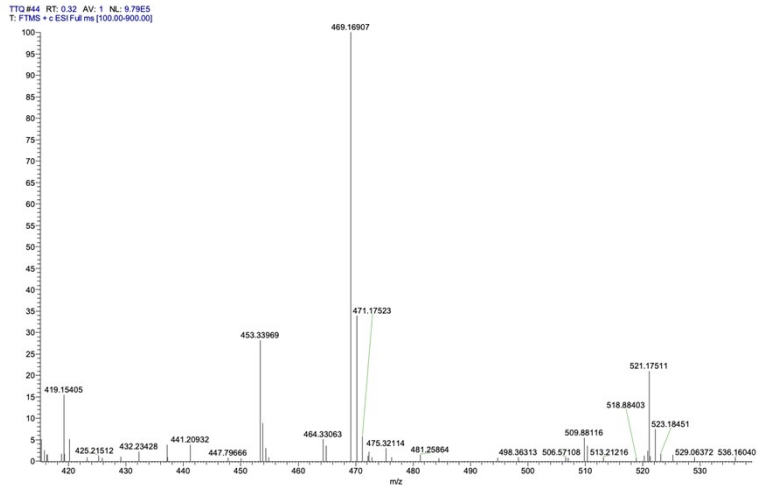

Fig. S11. High resolution mass spectrometry for **TTP.**

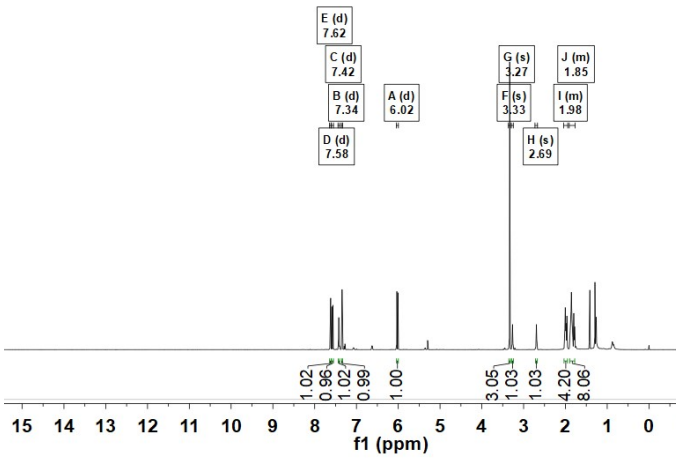

Fig. S12. ^{1}H NMR spectrum of **APT** in $CDCl_3$.

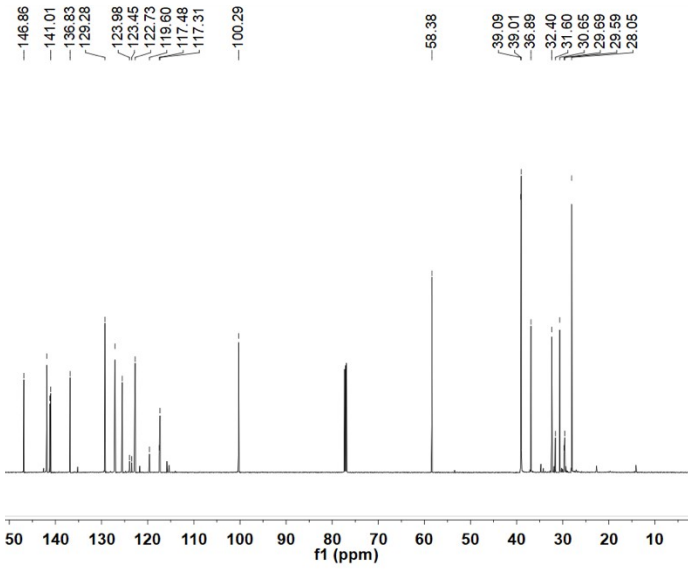

Fig. S13. ^{13}C NMR spectrum of **APT** in $CDCl_3$.